Supporting Information

Benzodithiophene Bridged Dimeric Perylene Diimide Amphiphile as Efficient Solution-Processed Non-Fullerene Small Molecule

Bo Jiang, [†a] Xin Zhang, [†a] Chuanlang Zhan, [a]* Zhenhuan Lu, [a] Jianhua Huang, [a] Xunlei Ding, [b] Shenggui He, [b] and Jiannian Yao[a]*

[†] Beijing National Laboratory for Molecular Sciences, CAS Key Laboratory of Photochemistry, Institute of Chemistry, Chinese Academy of Sciences, Beijing 100080, P. R. China. Tel/Fax: +86-10-82616517/82617312, E-mail: (C.Z.) clzhan@iccas.ac.cn , (J.Y.) jnyao@iccas.ac.cn .

[‡] Beijing National Laboratory for Molecular Sciences, State Key Laboratory for Structural Chemistry of Unstable and Stable Species, Institute of Chemistry, Chinese Academy of Sciences, Beijing, 100190, P. R. China.

Contents

1. Experimental section

1.1. Materials

All reagents and chemicals were purchased from commercial sources (TCI, Acros, Sigma, or Alfa) and used without further purification except statements. Solvents (toluene and tetrahydrofuran) were distilled by standard procedures before used for organic synthesis.

1.2. Instruments and measurements

^{1}H NMR and ^{13}C NMR spectrums were recorded by a Bruker DMX-400 spectrometer with $CDCl_3$ as a solvent and tetramethylsilane as an internal reference. MALDI-TOF mass spectra were recorded by a Bruker BIFLEXIII. Absorption spectra were taken on a Hitachi U-3010 UV-vis spectrophotometer. The pristine films on quartz plate used for the UV measurements were prepared by spin-coating a 10 mg/mL chloroform solution of the samples. The blending films used for absorption spectrum measurements were prepared on quartz plate under the same conditions (e.g. donor/acceptor ratio, spin-coating speed, solvent) to the preparation of photovoltaic devices that afford the best performances. The electrochemical cyclic voltammetry (CV) was performed using a Zahner IM6e electrochemical workstation in a 0.1 mol/L tetrabutylammonium hexafluorophosphate (Bu_4NPF_6) dichloromethane (DCM) solution with a scan speed at 0.1 V/s. A Pt wire and Ag/AgCl were used as the counter and reference electrodes, respectively. The concentration of **Bis-PDI-BDT-EG 1** and **2** is adjusted as 1×10^{-4} mol/L in chromatographic pure DCM solution) for the measurements cyclic voltammetry (CV). Thermogravimetric analysis (TGA) was performed on a Perkin-Elmer TGA-7 at a heating rate of 10℃/min under nitrogen flow. Atom force microscopy (AFM) was investigated by Brucker Multimode 8 using tapping-mode with a scan speed of 1Hz. X-ray diffraction (XRD) samples of pristine P3HT or blending films were prepared by spin-casting of solutions on silica slides. The XRD pattern was recorded by a Rigaku D/max–2500 diffractometer operated at 40 kV voltage and a 200 mA current with Cu Kα radiation.

1.3. Quantum chemical calculations

Computational details are presented as follows: Density functional theory (DFT) calculations were performed using the Gaussian 03 program[1] with the B3LYP exchange-correlation functional.[2] All-electron triple-ξ valence basis sets with polarization functions (6-311G**)[3] are used for all atoms. Geometry optimizations were performed with full relaxation of all atoms. Calculations were performed in gas phase without solvent effects. Vibrational frequency calculations were performed to check that the stable structures had no imaginary frequency. Charge distribution of the molecules was calculated by Mulliken population analysis, and the results by natural population analysis were found to be similar.

1.4. Fabrication and characterizations of OSCs

OSCs with a typical configuration of ITO/PEDOT: PSS/ **P3HT:PDI dimer** /Ca/Al was fabricated as follows. The ITO glass was pre-cleaned with deionized water, CMOS grade acetone and isopropanol in turn for 15 min. The organic residues were further removed by treating with

UV-ozone for 1 h. Then the ITO glass was modified by spin-coating PEDOT: PSS (poly(3,4-ethylenedioxythiophene)- poly(styrenesulfonate) layer, 30 nm) on it. After the ITO glasses were dried in oven at 150℃ for 15 min, the active layer was spin-coated on the ITO/PEDOT:PSS using a blend solution of **P3HT** and **PDI** dimer (40 mg/mL in o-dichlorobenzene (ODCB) for **1**, variants with donor/acceptor weight ratio, respectively). Ca (20 nm) and Al (80 nm) electrode was then subsequently thermally evaporated on the active layer under the vacuum of 1×10^{-6} Torr. The active area of the device was 0.06 cm^2, and the thickness of the active films were ～300 nm. The devices were characterized in nitrogen atmosphere under the illumination of simulated AM 1.5 G, 100 mW/cm^2 using a xenon-lamp-based solar simulator. The current-voltage (*I-V*) measurement of the devices was conducted on a computer-controlled Keithley 2400 Source Measure Unit. The EQE measurements of the encapsulated devices were performed in air (PV Measurements Inc., Model QEX7).

1.5. Measurements of the hole mobility by the space-charge limited current (SCLC) method.

The devices were fabricated with a configuration of ITO/PEDOT : PSS (30nm) / P3HT:PDI dimer(~300nm) /Au(600nm). The active layers were spin-coated under the conditions that afford the best photovoltaic results. The following equation was applied to estimate the hole mobilities:

$$J=9/8\varepsilon\varepsilon_0\mu_h V^2/L^3 exp[0.89(V/E_0L)^{0.5}] \quad (1)$$

where ε is the average dielectric constant of the blended film (here, ε is taken as 3.0 typically for polymers), ε_0 the permittivity of the vacuum, μ_h the zero-field mobility, E_0 the characteristic field, J the current density, L the thickness of the films, and $V = V_{appl}-V_{bi}$; V_{appl} the applied potential, and V_{bi} the built-in potential which results from the difference in the work function of the anode and the cathode (in this device structure, V_{bi} = 0.2 V). The results are plotted as $\ln(JL^3/V^2)$ vs $(V/L)^{0.5}$, as shown in Figure S7. The hole mobility of the blending films was deduced from the intercept value of $\ln(9\varepsilon\varepsilon_0\mu_0/8)$.

1.6. Measurements of the electron mobility by the space-charge limited current (SCLC) method.

The devices were fabricated with a configuration of ITO/titanium (diisopropoxide) bis(2,4-pentanedionate)[4c] (TIPD, 20nm) / P3HT:PDI dimer(~300nm) /Al(1000nm). Since the HOMO and LUMO energy levels of the TIPD were –3.91 eV and –6.0 eV, it can be used to fabricate the electron-only SCLC device. The TIPD buffer layer was prepared by spin-coating (3000 rpm) a 3.5 wt % TIPD isopropanol solution on the pre-cleaned ITO substrate and then baked at 150 °C for 10 min. Subsequently, the blended films were prepared using the same condition as the preparation of the best OSC device. Finally, a 1000 nm Al layer was thermally deposited on the top of the blended films in vacuum. Electron mobilities were extracted by fitting the current density–voltage curves using the Mott–Gurney relationship (space charge limited current) as follows:

$$J=9/8\varepsilon\varepsilon_0\mu_e V^2/L^3 exp[0.89(V/E_0L)^{0.5}] \quad (1)$$

where ε is the average dielectric constant of the blended film (here, ε is taken as 3.0 typically for polymers), ε_0 the permittivity of the vacuum, μ_e the zero-field mobility, E_0 the characteristic field, J the current density, L the thickness of the films, and $V = V_{appl}-V_{bi}$; V_{appl} the applied potential, and V_{bi} the built-in potential which results from the difference in the work function of the anode and the cathode (in this device structure, V_{bi} = 0.1 V). The results are plotted as $\ln(JL^3/V^2)$ vs $(V/L)^{0.5}$, as shown in Figure S8. The electron mobility of the blending films was deduced from the intercept value of $\ln(9\varepsilon\varepsilon_0\mu_0/8)$.

Following shows the chemical structure of TIPD.

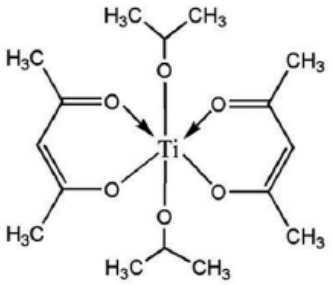

TIPD

2. Supporting figures

Figure S1. The TGA curves of **Bis-PDI-T-EG 1** and **2**

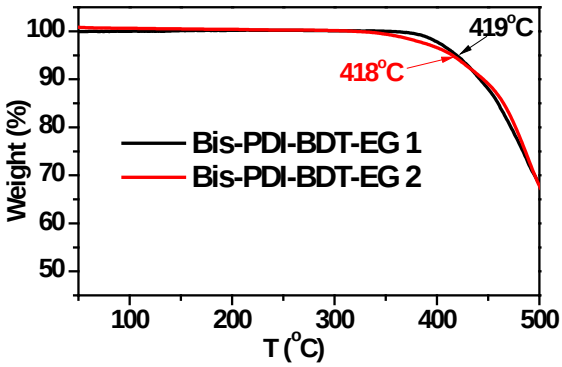

Figure S2. The optimal conformation of **Bis-PDI-T-EG** and the dihedral angles shown in the following Figures: Upper (**1**) and lower (**2**).

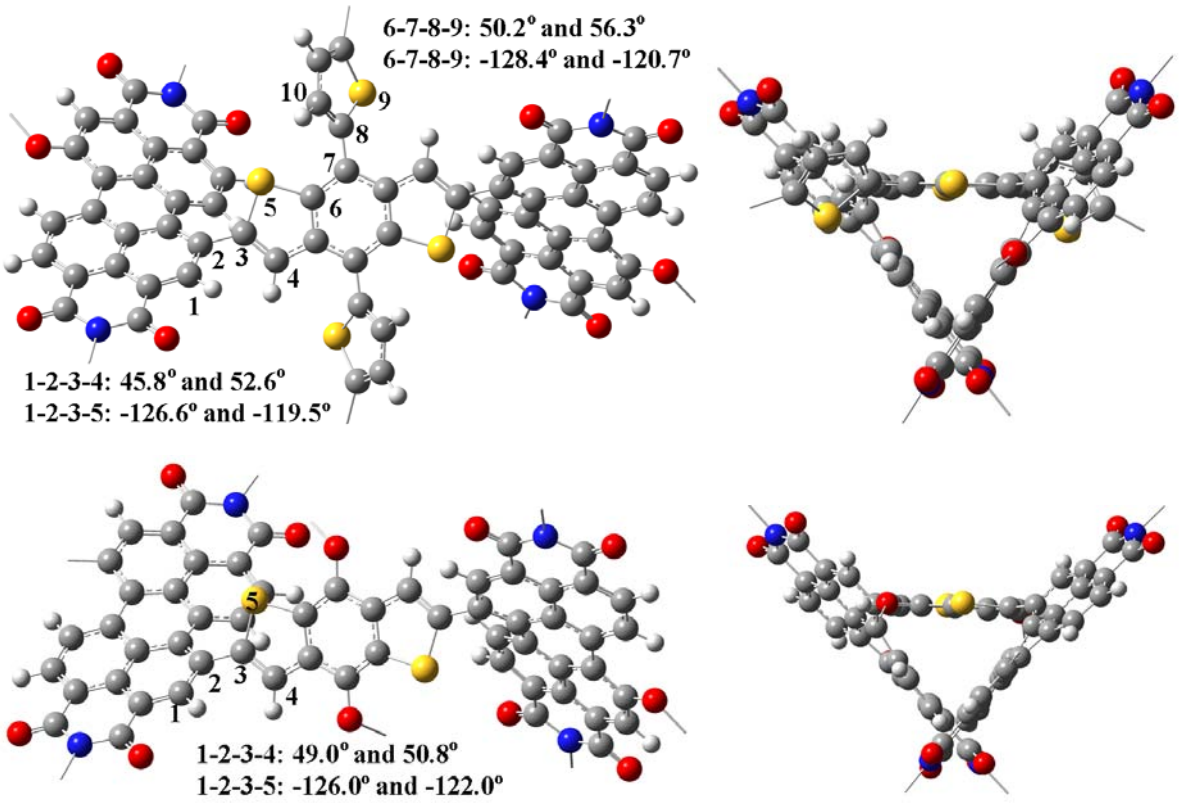

Noted: The dihedral angles along the selected atoms are shown in the figures. The two angles of 1-2-3-4 or 1-2-3-5 represent the dihedral angle between the BDT unit and that attached naphthalene unit for both the PDI units. The two angles of 6-7-8-9 or 6-7-8-10 represent the dihedral angle between the BDT unit and the attached thienyl unit at the 4- or 8-position.

Figure S3. The XRD patterns of the pure films of dimers **1** (blue) and **2** (black).

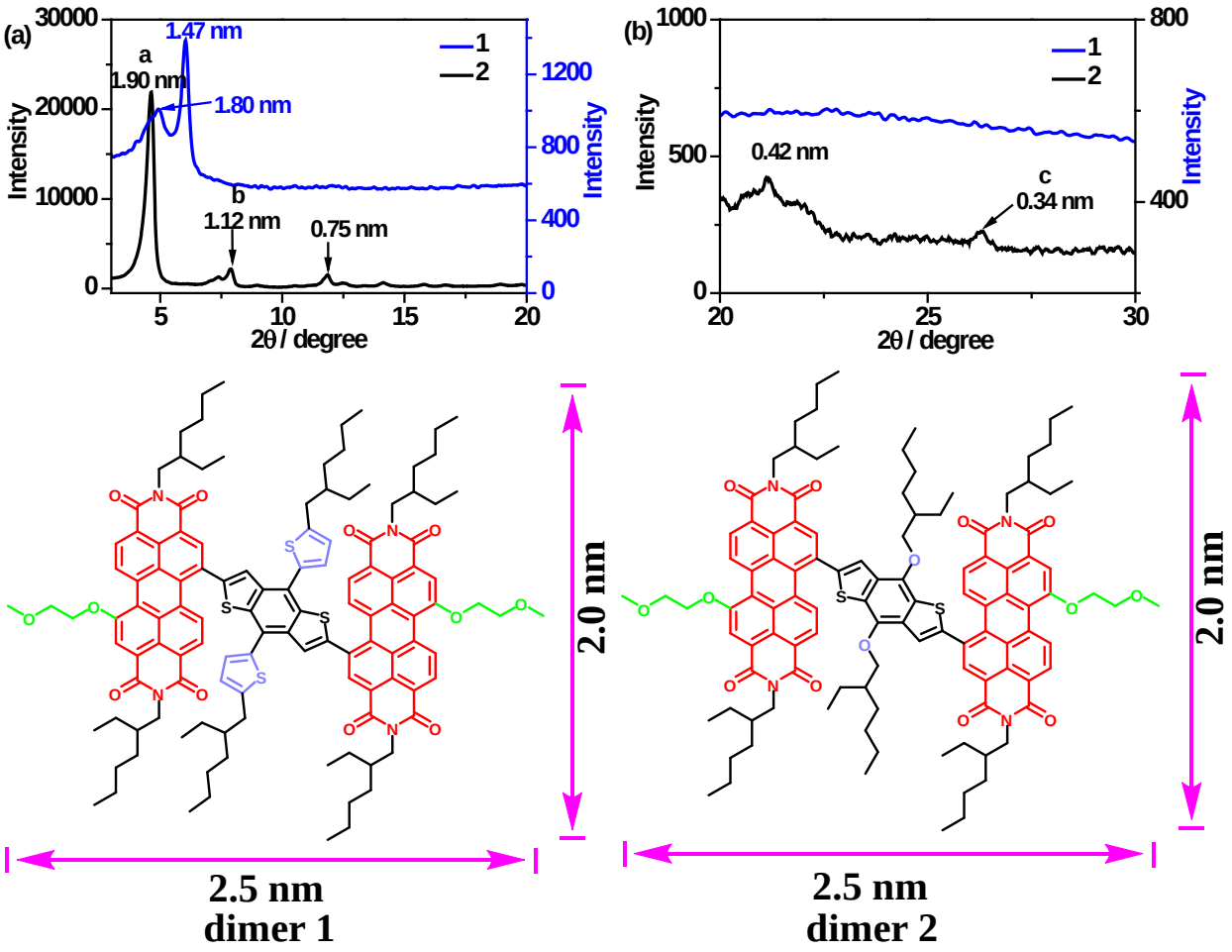

Figure S4. Cyclic voltammogram of **Bis-PDI-BDT-EG 1** and **2** (a) and P3HT (b) in a 0.1mol L^{-1} Bu_4NPF_6/CH_2Cl_2 solution with a scan rate of 100 mV s^{-1} and using Ag/AgCl as the reference electrode.

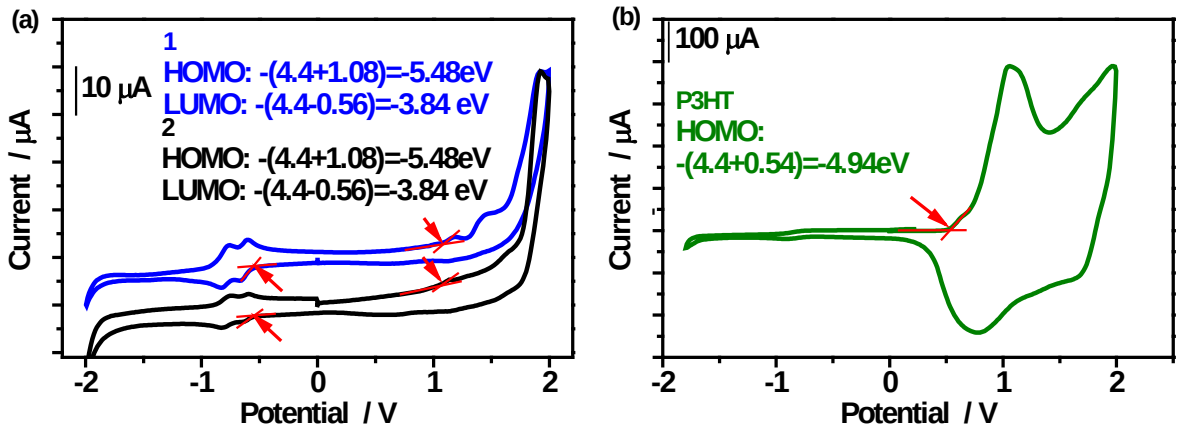

Figure S5. The *J*-*V* curve of dimer **2**: P3HT device which was fabricated from the chloroform solution with an overall concentration of 10 mg ml^{-1} and a D/A ratio of 1:1.

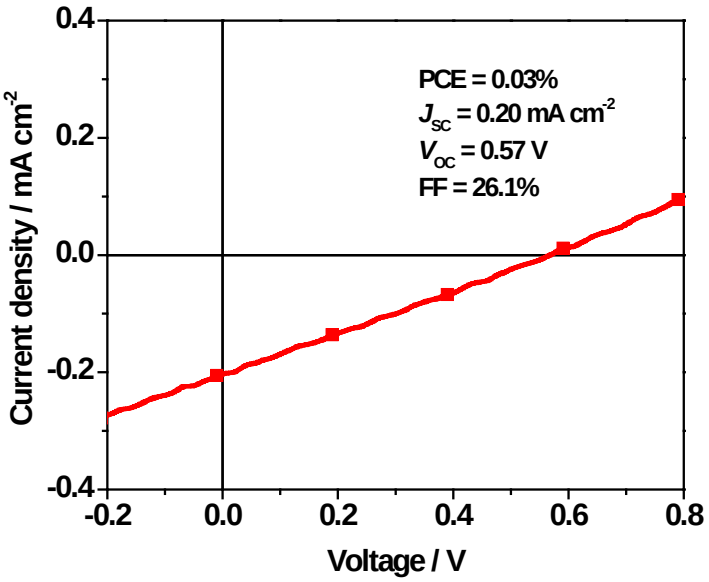

As comparisions, the OSC devices based on dimer **2** as the acceptor material and P3HT as the donor material were fabricated. Dimer **2** shows over-strong aggregation ability, severely limited solubility (< 1 mg ml^{-1}) and very poor solution-processability using the common organic solvents such as dichloromethane (DCM), chloroform, tetrahydrofuran (THF), chlorobenzene, 1,2-dichlorobenzene (o-DCB) and toluene. To fabricate the solution-processed OSC devices with dimer **2** as the acceptor material, the most commonly used solvent of chloroform was chosen to dissolve the D/A blend under the weight ratio of 1:1 with an overall concentration of 10 mg ml^{-1}. After stirring 3 hours, the BHJ OSC devices were fabricated. As expected, the resulted devices displayed very poor photon-to-electron conversion, only with a PCE of 0.03%.

Figure S6. Plots of $\ln(JL^3/V^2)$ vs. $(V/L)^{0.5}$ of **Bis-PDI-T-EG 1**, extracted from the hole-only SCLC curves under different conditions. The film thicknesses are displayed in the embedded textboxes.

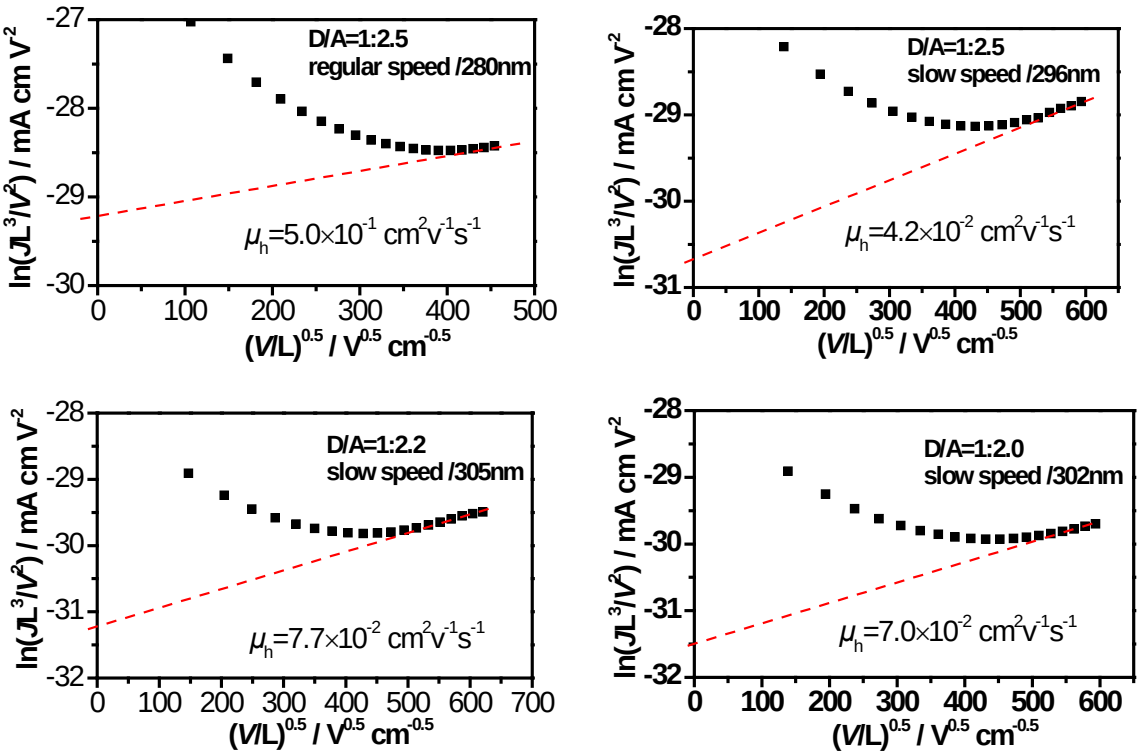

Figure S7. Plots of $\ln(JL^3/V^2)$ vs. $(V/L)^{0.5}$ of **Bis-PDI-T-EG 1**, extracted from the electron-only SCLC curves under different conditions.

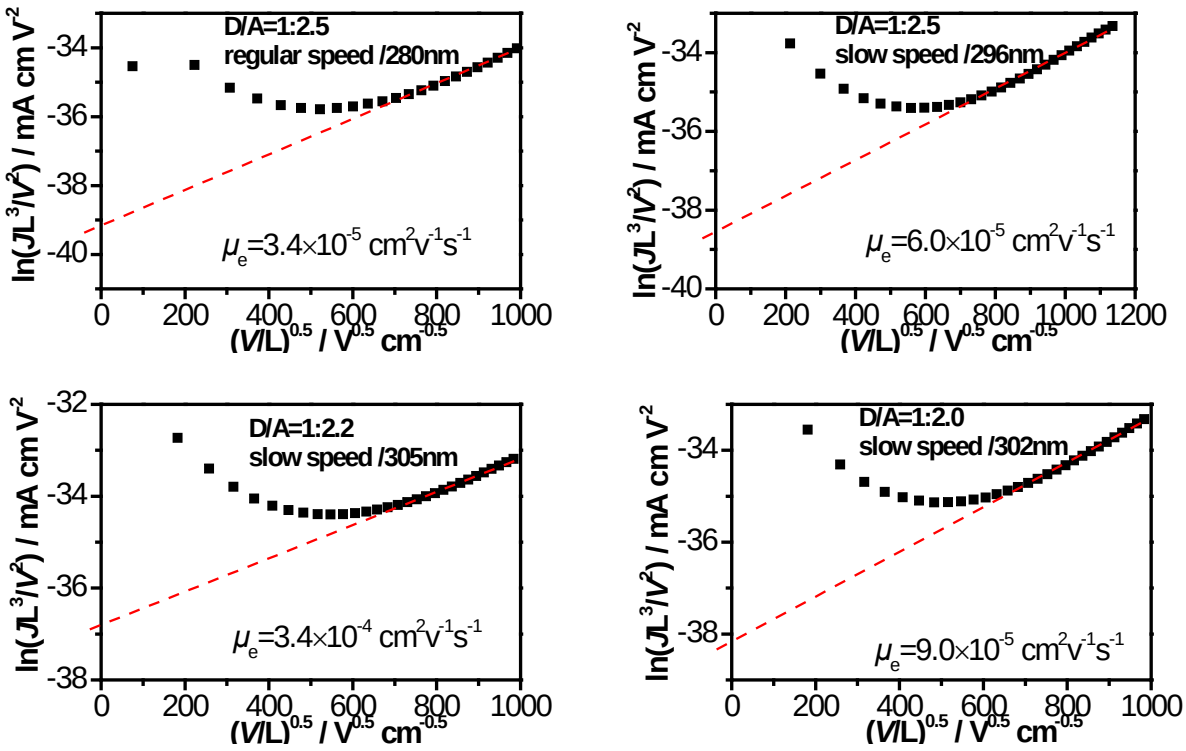

Figure S8. The absorption spectra of the pure films of P3HT (black) and **1** (red).

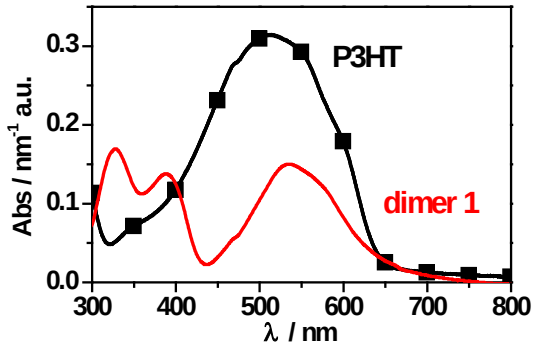

Figure S9. XRD patterns of the blended P3HT:**1** films with D/A=1:2.5 (red), 1:2.2 (olive), and 1:2.0 (orange) prepared under slow-speed conditions. As comparisons, the XRD patterns of the pristine P3HT (black) and **1** (blue) are also shown.

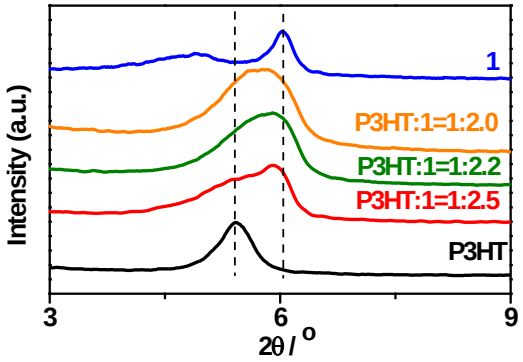

Figure S10. Tapping-mode AFM height and phase images of the blended films P3HT: **1** with different D/A ratios: (A), D/A=1/1 (w/w); (B), D/A=1/4 (w/w).

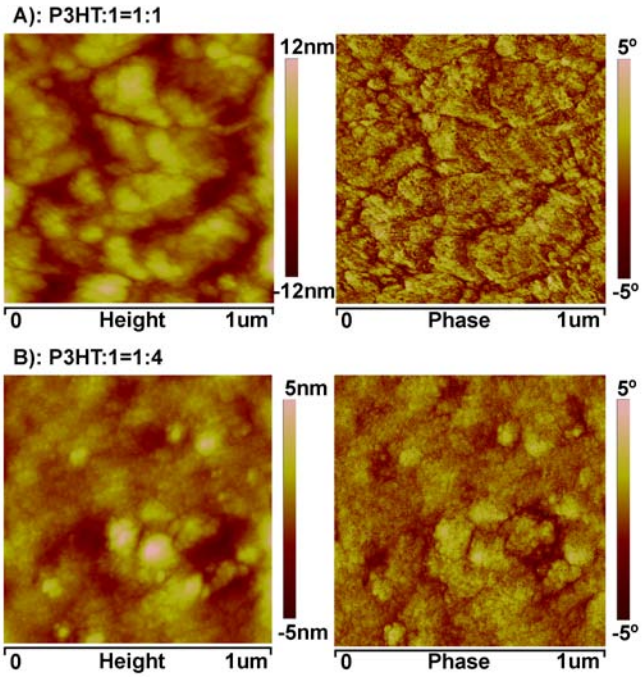

Comparisons of the AFM height and phase images from different D/A ratios of 1:1 and 1:4, it is seen that increasing the weight percentage of acceptor material, **1**, the bright phases became more dispersed and the domain size became smaller. This suggests that the bright phases are mainly contributed from the electron donor material of P3HT. Accordingly, the dark phases are mainly from the electron-acceptor material.

Figure S11. Tapping-mode AFM height images of the champion P3HT: 1 based devices prepared under different conditions: (A), D/A=1/2.5 (w/w), regular-speed; (B), D/A=1/2.5 (w/w), slow-speed; and (C), D/A=1/2.2 (w/w), slow-speed.

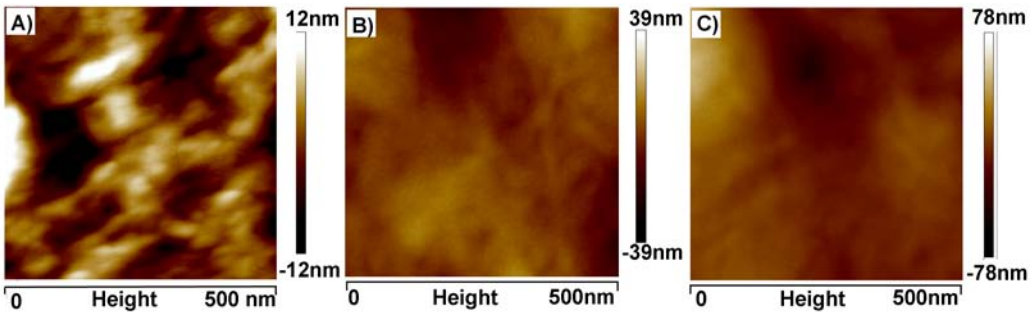

3. Supporting tables

Table S1. Device datas based on P3HT:**D1** at various D/A ratios

D/A ratio [w/w]	V_{OC} [V]	J_{SC} [mA cm^{-2}]	FF	PCE [%] best	PCE [%] ave.[c)]
2:1[a)]	0.63	1.95	0.38	0.47	0.43
1:1[a)]	0.64	3.77	0.38	0.92	0.89
1:2[a)]	0.66	4.75	0.46	1.46	1.39
1:2.5[a)]	0.67	4.88	0.53	1.72	1.66
1:3[a)]	0.69	4.42	0.48	1.47	1.30
1:4[a)]	0.69	3.38	0.51	1.19	1.14
2:1 [b)]	0.65	5.21	0.32	1.08	1.03
1:1 [b)]	0.65	5.07	0.33	1.18	1.15
1:2[b)]	0.68	5.69	0.50	1.93	1.84
1:2.2[b)]	0.68	5.83	0.49	1.95	1.87
1:2.5[b)]	0.69	5.48	0.49	1.87	1.81
1:2.8[b)]	0.68	5.44	0.50	1.83	1.78
1:3 [b)]	0.68	5.46	0.49	1.82	1.78
1:4 [b)]	0.67	5.15	0.45	1.56	1.50

[a)]Regular-speed. [b)]Slow-speed. [c)]Average values over ten devices.

4. NMR spectra of Bis-PDI-T-EG 1 and 2

^{1}H NMR spectrum of **1**

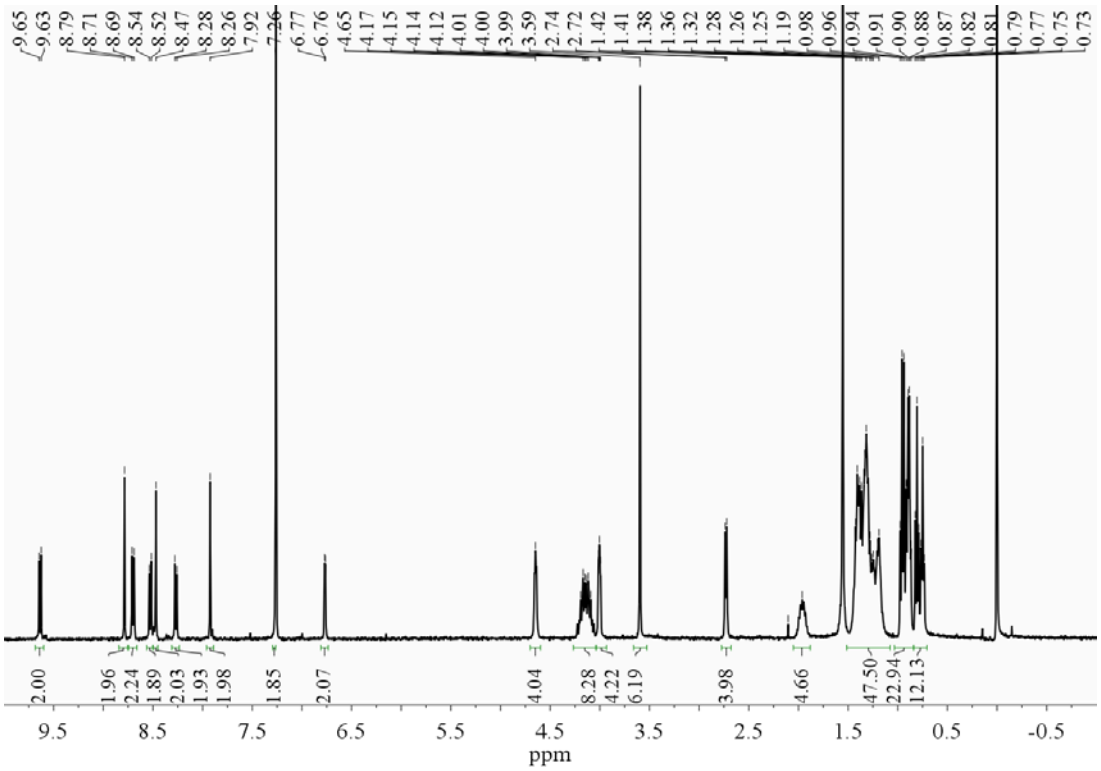

^{13}C NMR spectrum of **1**

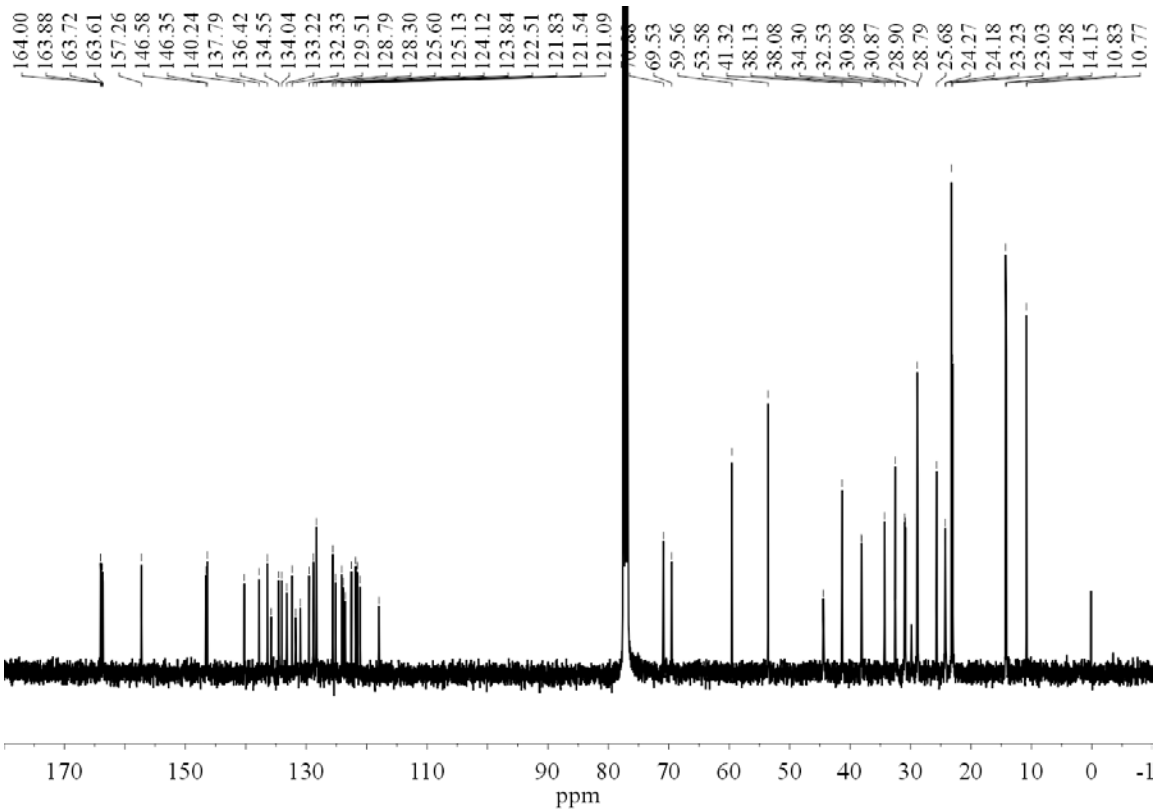

^{1}H NMR spectrum of **2**

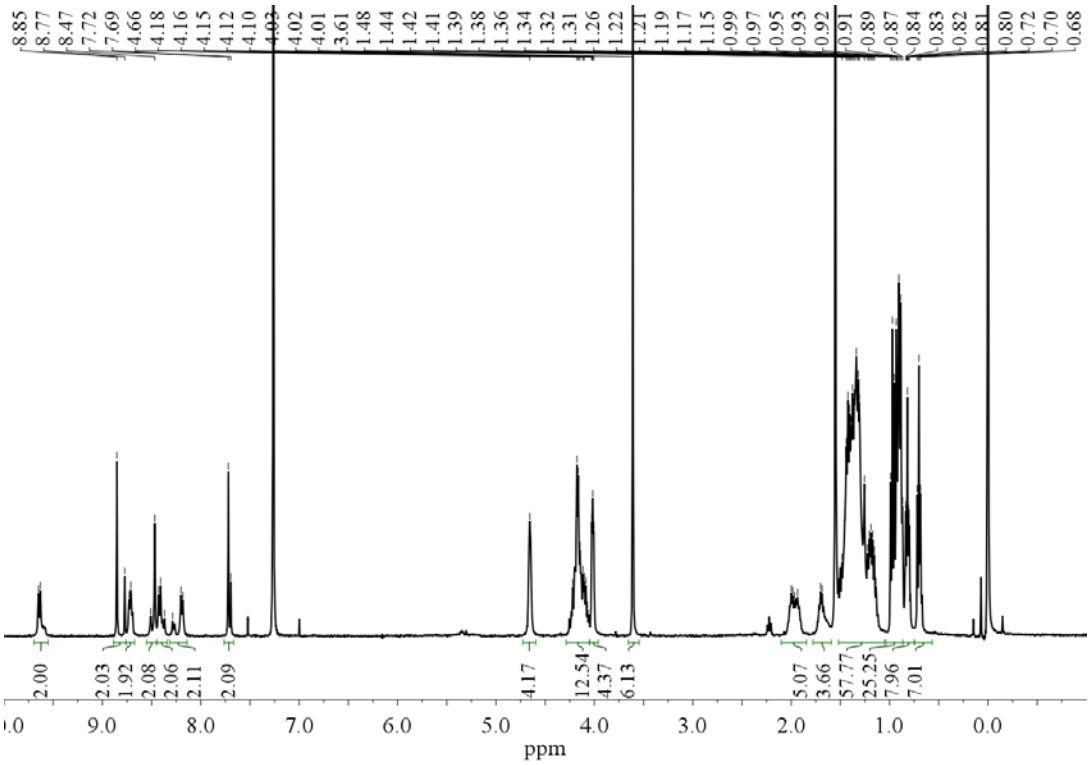

5. References

1. M. J. Frisch, G. W. Trucks, H. B. Schlegel, G. E. Scuseria, M. A. Robb, J. R. Cheeseman, J. A. Montgomery Jr., T. Vreven, K. N. Kudin, J. C. Burant, J. M. Millam, S. S. Iyengar, J. Tomasi, V. Barone, B. Mennucci, M. Cossi, G. Scalmani, N. Rega, G. A. Petersson, H. Nakatsuji, M. Hada, M. Ehara, K. Toyota, R. Fukuda, J. Hasegawa, M. Ishida, T. Nakajima, Y. Honda, O. Kitao, H. Nakai, M. Klene, X. Li, J. E. Knox, H. P. Hratchian, J. B. Cross, V. Bakken, C. Adamo, J. Jaramillo, R. Gomperts, R. E. Stratmann, O. Yazyev, A. J. Austin, R. Cammi, C. Pomelli, J. W. Ochterski, P. Y. Ayala, K. Morokuma, G. A. Voth, P. Salvador, J. J. Dannenberg, V. G. Zakrzewski, S. Dapprich, A. D. Daniels, M. C. Strain, O. Farkas, D. K. Malick, A. D. Rabuck, K. Raghavachari, J. B. Foresman, J. V. Ortiz, Q. Cui, A. G. Baboul, S. Clifford, J. Cioslowski, B. B. Stefanov, G. Liu, A. Liashenko, P. Piskorz, I. Komaromi, R. L. Martin, D. J. Fox, T. Keith, M. A. Al-Laham, C. Y. Peng, A. Nanayakkara, M. Challacombe, P. M. W. Gill, B. Johnson, W. Chen, M. W. Wong, C. Gonzalez, J. A. Pople, Gaussian 03, Revision C.02, Gaussian, Inc., Wallingford CT, 2004.
2. a) C. T. Lee, W. T. Yang, R. G. Parr, *Phys. Rev.* B 1988, **37**, 785-789; (b) A. D. Becke, *J. Chem. Phys.* 1993, **98**, 5648-5652.
3. Krishnan, R.; Binkley, J. S.; Seeger, R.; Pople, J. A. *J. Chem. Phys.* 1980, 72, 650-654.
4. (a) T. Y. Chu, O. K. Song, *Appl. Phys. Lett*. 2007, **90**, 203512; (b) G. G. Malliaras, J. R. Salem, P. J. Brock, C. Scott, *Phys. Rev. B* 1998, ***58***, 13411.
5. (a) J. Huang, Y.Zhao, X. Ding, H. Jia, B. Jiang, Z. Zhang, C. Zhan, S. He, Q. Pei, Y. Li, Y. Liu, and J. Yao, *Polym. Chem.*, 2012, **3**, 2170-2177; (b) J. Huang, Y. Zhao, W. He, H. Jia, Z. Lu, B. Jiang, C. Zhan, Q. Pei, Y. Liu and J. Yao, *Polym. Chem.*, 2012, **3**, 2832-2841; (c) J. Huang, H. Jia, L. Li, Z. Lu, W. Zhang, W. He, B. Jiang, A. Tang, Z. A. Tan, C. Zhan, Y. Li and J. Yao, *Phys. Chem. Chem. Phys.*, 2012, **14**, 14238-14242.